

Emergence of molecular-type characteristic spectrum of hidden-charm pentaquark with strangeness embodied in the $P_{\psi_s}^\Lambda(4338)$ and $P_{cs}(4459)$

Fu-Lai Wang^{1,2,3*} and Xiang Liu^{1,2,3†}

¹*School of Physical Science and Technology, Lanzhou University, Lanzhou 730000, China*

²*Research Center for Hadron and CSR Physics, Lanzhou University
and Institute of Modern Physics of CAS, Lanzhou 730000, China*

³*Lanzhou Center for Theoretical Physics, Key Laboratory of Theoretical Physics of Gansu Province,
and Frontiers Science Center for Rare Isotopes, Lanzhou University, Lanzhou 730000, China*

Inspired by the newly observed $P_{\psi_s}^\Lambda(4338)$ and the reported $P_{cs}(4459)$, we indicate the existence of the molecular-type characteristic mass spectrum for hidden-charm pentaquark with strangeness. It shows that the $P_{cs}(4459)$ may contain two substructures corresponding to the $\Xi_c \bar{D}^*$ molecular states with $J^P = 1/2^-$ and $3/2^-$, while there exists the corresponding $\Xi_c \bar{D}$ molecular state with $J^P = 1/2^-$. As the prediction, we present another characteristic mass spectrum of the $\Xi_c' \bar{D}^*$ molecular states. Experimental confirmation of these characteristic mass spectra is a crucial step of constructing hadronic molecular family.

I. INTRODUCTION

Since the birth of the quark model [1, 2], the concept of exotic hadronic matter has been proposed, which has attracted extensive attention from both experimentalists and theorists. Especially, with the accumulation of experimental data, the observations of charmonium-like XYZ states and P_c states in the past around twenty years make this issue becomes hot spot of hadron physics up till now [3–13]. These studies are helpful to deepen our understanding of non-perturbative quantum chromodynamics (QCD). Among different exotic hadronic matters, the hadronic molecular state was popularly applied to explain these novel phenomena relevant to new hadronic states since most of observed hadronic states are close the thresholds of hadron pair. A typical example is the LHCb's discoveries of the $P_c(4312)$, $P_c(4440)$, and $P_c(4457)$ in the $J/\psi p$ invariant mass spectrum of the $\Lambda_b \rightarrow J/\psi p K$ [14] weak decay, which show a characteristic mass spectrum consistent with that of hidden-charm molecular pentaquark, which was predicted in Refs. [15–21]. Finally, it provides strong evidence to support the existence of the hidden-charm meson-baryon molecular states. Of course, there also exist other possible interpretations to the $P_c(4312)$, $P_c(4440)$, and $P_c(4457)$ [3–13, 22].

Very recently, the LHCb Collaboration announced the observed of a $J/\psi \Lambda$ resonance in the $B^- \rightarrow J/\psi \Lambda \bar{p}$ process [23], which has resonance parameters

$$M = 4338.2 \pm 0.7 \pm 0.4 \text{ MeV}, \quad \Gamma = 7.0 \pm 1.2 \pm 1.3 \text{ MeV},$$

and significance larger than 10σ . Thus, this $J/\psi \Lambda$ resonance is referred to be the $P_{\psi_s}^\Lambda(4338)$, which is the candidate of hidden-charm pentaquark with strangeness, as predicted by former theoretical studies [24–50]. Before

observing the $P_{\psi_s}^\Lambda(4338)$, LHCb once reported an evidence of the enhancement structure ($P_{cs}(4459)$) in the $J/\psi \Lambda$ invariant mass spectrum of the $\Xi_b^- \rightarrow J/\psi \Lambda K$ [51], which is the candidate of hidden-charm pentaquark with strangeness [24–50].

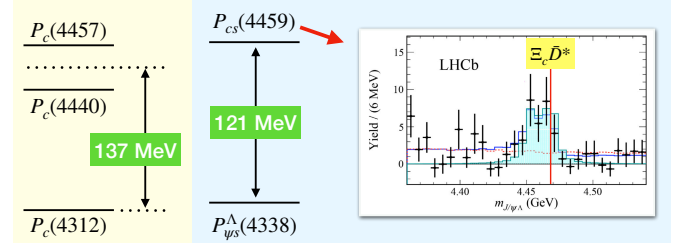


FIG. 1. Comparison of the mass spectrum of three P_c states [14] and that of the $P_{\psi_s}^\Lambda(4338)$ [23] and $P_{cs}(4459)$ [51]. Here, we also list the experimental data of the $P_{cs}(4459)$ from LHCb [51].

In this work, we indicate that there exists a new characteristic mass spectrum applied to identify the molecular-type hidden-charm pentaquark with strangeness, which is inspired by the observed $P_{\psi_s}^\Lambda(4338)$ and the reported $P_{cs}(4459)$. As shown in Fig. 1, the gap between the $P_c(4312)$ mass and the average mass of the $P_c(4440)$ and $P_c(4457)$ is 137 MeV, which is similar to the mass gap of the $P_{cs}(4459)$ and the $P_{\psi_s}^\Lambda(4338)$. This is analogous to the similarity of the mass gaps for the ω and ϕ meson families [52]. We also notice an interesting phenomenon, and there exists corresponding relations of these P_c and P_{cs} states, i.e., the $P_{\psi_s}^\Lambda(4338)$ should correspond to the $P_c(4312)$, while the $P_{cs}(4459)$ structure corresponds to the $P_c(4440)$ and $P_c(4457)$. This fact makes us conjecture that the $P_{cs}(4459)$ enhancement structure should contain two substructures. If checking the LHCb data of the $J/\psi \Lambda$ invariant mass spectrum of the $\Xi_b^- \rightarrow J/\psi \Lambda K$ [51], we find that there exists possible double peak structure slightly below the $\Xi_c \bar{D}^*$ threshold as indicated in Fig. 1, which just correspond to the $\Xi_c \bar{D}^*$

* wangfl2016@lzu.edu.cn

† xiangliu@lzu.edu.cn

molecular states with $J^P = 1/2^-$ and $3/2^-$. Such scenario can be tested in future experiment like the LHCb. As the partner of $P_c(4312)$, the $\Xi_c \bar{D}$ molecular state with $J^P = 1/2^-$ was studied in this work. We should indicate the fact that the central value of the mass of the newly reported $P_{\psi_s}^\Lambda(4338)$ is above the $\Xi_c \bar{D}$ threshold, which is the difficulty to directly assign the newly observed $P_{\psi_s}^\Lambda(4338)$ as the $\Xi_c \bar{D}$ molecular state with $J^P = 1/2^-$. How to solving this puzzling phenomenon is also an interesting topic. In the final section, we will address this point. Inspired by the established molecular-type characteristic mass spectrum of three P_c states in 2019 [14] and the molecular-type characteristic mass spectrum of the $P_{\psi_s}^\Lambda(4338)$ and the $P_{cs}(4459)$ enhancement structure found in this work, we further give a new characteristic mass spectrum of the $\Xi_c' \bar{D}^{(*)}$ molecular states, which will be accessible at experiment.

This paper is organized as the follows. After introduction, the calculation of the interactions of these discussed $\Xi_c^{(\prime)} \bar{D}^{(*)}$ systems will be given by adopting the OBE model in Sec. II. With this preparation, we discuss the characteristic mass spectra of the $\Xi_c^{(\prime)} \bar{D}^{(*)}$ molecular pentaquarks in Sec. III. Finally, we will give the discussion and conclusion in Sec. IV.

II. THE OBE EFFECTIVE POTENTIALS OF THE $\Xi_c^{(\prime)} \bar{D}^{(*)}$ SYSTEMS

For getting the information of the interactions of the $\Xi_c^{(\prime)} \bar{D}^{(*)}$ systems, the one-boson-exchange (OBE) model is adopted. In the OBE model, the interaction between two hadrons is a direct consequence of the exchange of the allowed light mesons [5, 10], which is one of the effective ways to investigate the interactions between hadrons. Such a formalism is a straightforward extension of the traditional meson exchange model involved in the nuclear force [53]. Up to now, the OBE model has successfully applied the exploration of a series of hadronic molecular states including the P_c states and the T_{cc} state [5, 10]. We should indicate that it is not the only way to get the interactions between hadrons, since there also exist other approaches like the chiral effective field theory [12]. For the chiral effective field theory, the contact term is usually introduced, which is different from the treatment of the OBE model on this point. In fact, this difference reflects the different treatment to the short distant interactions between hadrons under two approaches. Despite all this, the OBE model and the chiral effective field theory usually can reach the same conclusion for the same hadronic molecular states.

In general, there exists three typical steps for deducing the effective potentials of these discussed $\Xi_c^{(\prime)} \bar{D}^{(*)}$ systems within the OBE model. As the first step, we should write out the scattering amplitudes $\mathcal{M}(h_1 h_2 \rightarrow h_3 h_4)$ of the scattering processes $h_1 h_2 \rightarrow h_3 h_4$ by considering the effective Lagrangian approach.

According to the heavy quark spin symmetry, the hadrons containing single heavy quark with total spin $J_\pm = j_l \pm 1/2$ (except $j_l = 0$) come into doublets, which can be written as the super-fields when constructing the compact effective Lagrangians. For the pseudoscalar anti-charmed meson \bar{D} with $I(J^P) = 1/2(0^-)$ and vector anti-charmed meson \bar{D}^* with $I(J^P) = 1/2(1^-)$, they are degenerated in the heavy quark spin symmetry, which can be written as the super-field $H_a^{(\bar{Q})} = (\bar{D}_a^{*(\bar{Q})\mu} \gamma_\mu - \bar{D}_a^{(\bar{Q})} \gamma_5) \frac{(1-\not{v})}{2}$ [54]. In the heavy quark limit, the charm baryons can be classified in terms of the flavor symmetry of the diquark, the spin of the charm baryon in the 6_F flavor representation is either $1/2$ or $3/2$, while the spin of the charm baryon in the 3_F flavor representation is only $1/2$. Here, we need to mention that Ξ_c with $J^P = 1/2^+$ denotes the S -wave charm baryon in 3_F flavor representation, while Ξ_c' with $J^P = 1/2^+$ is the S -wave charmed baryon in 6_F flavor representation. The involved effective Lagrangians for depicting the heavy hadrons $\mathcal{B}_c/\bar{D}^{(*)}$ coupling with the light scalar, pseudoscalar, and vector mesons read as [54–61]

$$\mathcal{L}_{\mathcal{B}_3 \mathcal{B}_3 \sigma} = l_B \langle \bar{\mathcal{B}}_3 \sigma \mathcal{B}_3 \rangle, \quad (1)$$

$$\mathcal{L}_{\mathcal{B}_3 \mathcal{B}_3 \mathbb{V}} = \frac{1}{\sqrt{2}} \beta_B g_V \langle \bar{\mathcal{B}}_3 v \cdot \mathbb{V} \mathcal{B}_3 \rangle, \quad (2)$$

$$\mathcal{L}_{\mathcal{B}_6 \mathcal{B}_6 \sigma} = -l_S \langle \bar{\mathcal{B}}_6 \sigma \mathcal{B}_6 \rangle, \quad (3)$$

$$\mathcal{L}_{\mathcal{B}_6 \mathcal{B}_6 \mathbb{P}} = i \frac{g_1}{2f_\pi} \varepsilon^{\mu\nu\lambda\kappa} v_\kappa \langle \bar{\mathcal{B}}_6 \gamma_\mu \gamma_\lambda \partial_\nu \mathbb{P} \mathcal{B}_6 \rangle, \quad (4)$$

$$\begin{aligned} \mathcal{L}_{\mathcal{B}_6 \mathcal{B}_6 \mathbb{V}} &= -\frac{\beta_S g_V}{\sqrt{2}} \langle \bar{\mathcal{B}}_6 v \cdot \mathbb{V} \mathcal{B}_6 \rangle \\ &\quad -i \frac{\lambda_S g_V}{3\sqrt{2}} \langle \bar{\mathcal{B}}_6 \gamma_\mu \gamma_\nu (\partial^\mu \mathbb{V}^\nu - \partial^\nu \mathbb{V}^\mu) \mathcal{B}_6 \rangle, \end{aligned} \quad (5)$$

$$\mathcal{L}_{\mathcal{B}_3 \mathcal{B}_6 \mathbb{P}} = -\sqrt{\frac{1}{3}} \frac{g_A}{f_\pi} \langle \bar{\mathcal{B}}_6 \gamma^5 (\gamma^\mu + v^\mu) \partial_\mu \mathbb{P} \mathcal{B}_3 \rangle + h.c., \quad (6)$$

$$\begin{aligned} \mathcal{L}_{\mathcal{B}_3 \mathcal{B}_6 \mathbb{V}} &= -\frac{\lambda_I g_V}{\sqrt{6}} \varepsilon^{\mu\nu\lambda\kappa} v_\mu \langle \bar{\mathcal{B}}_6 \gamma^5 \gamma_\nu (\partial_\lambda \mathbb{V}_\kappa - \partial_\kappa \mathbb{V}_\lambda) \mathcal{B}_3 \rangle \\ &\quad + h.c., \end{aligned} \quad (7)$$

$$\mathcal{L}_{\bar{D} \bar{D} \sigma} = -2g_\sigma \bar{D}_a \bar{D}_a^\dagger \sigma, \quad (8)$$

$$\mathcal{L}_{\bar{D}^* \bar{D}^* \sigma} = 2g_\sigma \bar{D}_{a\mu}^* \bar{D}_a^{*\mu\dagger} \sigma, \quad (9)$$

$$\mathcal{L}_{\bar{D}^* \bar{D}^* \mathbb{P}} = \frac{2ig}{f_\pi} v^\alpha \varepsilon_{\alpha\mu\nu\lambda} \bar{D}_a^{*\mu\dagger} \bar{D}_b^{*\lambda} \partial^\nu \mathbb{P}_{ab}, \quad (10)$$

$$\mathcal{L}_{\bar{D} \bar{D} \mathbb{V}} = \sqrt{2} \beta g_V \bar{D}_a \bar{D}_b^\dagger v \cdot \mathbb{V}_{ab}, \quad (11)$$

$$\begin{aligned} \mathcal{L}_{\bar{D}^* \bar{D}^* \mathbb{V}} &= -\sqrt{2} \beta g_V \bar{D}_{a\mu}^* \bar{D}_b^{*\mu\dagger} v \cdot \mathbb{V}_{ab} \\ &\quad -2\sqrt{2} i \lambda g_V \bar{D}_a^{*\mu\dagger} \bar{D}_b^{*\nu} (\partial_\mu \mathbb{V}_\nu - \partial_\nu \mathbb{V}_\mu)_{ab}. \end{aligned} \quad (12)$$

Here, $v_\mu = (1, \mathbf{0})$ is the four velocity under the non-relativistic approximation, and σ stands for the scalar singlet meson. Additionally, the matrices \mathcal{B}_3 , \mathcal{B}_6 , \mathbb{P} , and \mathbb{V}_μ have the standard forms as listed below

$$\mathcal{B}_3 = \begin{pmatrix} 0 & \Lambda_c^+ & \Xi_c^+ \\ -\Lambda_c^+ & 0 & \Xi_c^0 \\ -\Xi_c^+ & -\Xi_c^0 & 0 \end{pmatrix}, \quad (13)$$

$$\mathcal{B}_6 = \begin{pmatrix} \Sigma_c^{++} & \frac{\Sigma_c^+}{\sqrt{2}} & \frac{\Xi_c^{(\prime)+}}{\sqrt{2}} \\ \frac{\Sigma_c^+}{\sqrt{2}} & \Sigma_c^0 & \frac{\Xi_c^{(\prime)0}}{\sqrt{2}} \\ \frac{\Xi_c^{(\prime)+}}{\sqrt{2}} & \frac{\Xi_c^{(\prime)0}}{\sqrt{2}} & \Omega_c^0 \end{pmatrix}, \quad (14)$$

$$\mathbb{P} = \begin{pmatrix} \frac{\pi^0}{\sqrt{2}} + \frac{\eta}{\sqrt{6}} & \pi^+ \\ \pi^- & -\frac{\pi^0}{\sqrt{2}} + \frac{\eta}{\sqrt{6}} \end{pmatrix}, \quad (15)$$

$$\mathbb{V}_\mu = \begin{pmatrix} \frac{\rho^0}{\sqrt{2}} + \frac{\omega}{\sqrt{2}} & \rho^+ \\ \rho^- & -\frac{\rho^0}{\sqrt{2}} + \frac{\omega}{\sqrt{2}} \end{pmatrix}_\mu, \quad (16)$$

respectively.

As an effective way, the OBE model was widely used to investigate the interactions between hadrons. In calculation, the involved coupling constants are as input when discussing the problem of the hadronic molecular state. Usually, we prefer to fix the coupling constant if there exists the corresponding experimental data. For some coupling constants, we can estimate them by phenomenological models, where the relevant experimental information is absent. These coupling constants adopted in this work can be extracted from the experimental data or by the theoretical model, and the corresponding signs between these coupling constants can be fixed by the quark model [62]. Thus, we take $g_\sigma = 0.76$, $l_B = -3.65$, $l_S = 6.20$, $g = 0.59$, $g_4 = 1.06$, $g_1 = 0.94$, $f_\pi = 132$ MeV, $\beta_{g_V} = -5.25$, $\beta_B g_V = -6.00$, $\beta_S g_V = 12.00$, $\lambda_{g_V} = -3.27$ GeV⁻¹, $\lambda_I g_V = -6.80$ GeV⁻¹, and $\lambda_S g_V = 19.20$ GeV⁻¹ in the following numerical analysis [39, 61, 63]. Here, g_σ can be deduced by the relation $g_\sigma = \tilde{g}/2\sqrt{6}$ with $\tilde{g} = 3.73$ due to the spontaneously broken chiral symmetry [64]. The pion coupling constant g is determined by reproducing the experimental width of the $D^{*+} \rightarrow D^0 \pi^+$ process [65, 66]. According to the vector meson dominance mechanism, β and g_V are fixed [66, 67]. λ can be obtained by comparing the form factor obtained from the lattice QCD with this calculated via the light cone sum rule [66]. g_1 is related to another coupling constant g_4 by the relation $g_1 = \sqrt{8}g_4/3$ [68], and g_4 can be extracted by the decay width of the $\Sigma_c^* \rightarrow \Lambda \pi$ process. l_S is extracted with the chiral multiplet assumption [68]. For the coupling constants l_B , β_B , β_S , λ_I , and λ_S , we can calculate them by the quark model [62], which is a popular approach to determine the coupling constants. Here, for the discussed vertex, we can write out its amplitude at hadronic and quark levels. By connecting these two amplitudes, finally the coupling constant can be obtained. Here, we need to indicate that these coupling constants adopted in this work were applied to reproduce the masses of the observed three P_c states under the S -wave isoscalar $\Sigma_c \bar{D}^{(*)}$ molecular assignment [63].

With the above preparation, the obtained effective potentials in the momentum space can be related to the corresponding scattering amplitudes via the Breit approximation [69]. Finally, the effective potentials in the

coordinate space can be obtained by the Fourier transformation. Since the discussed hadrons are not pointlike particles, we should introduce the monopole type form factor $\mathcal{F}(q^2, m_E^2) = (\Lambda^2 - m_E^2)/(\Lambda^2 - q^2)$ [70, 71] in each interaction vertex, which can compensate the effect from the off-shell exchanged mesons and depict the structure effect of interaction vertex.

In order to obtain the concrete effective potentials for these discussed hidden-charm molecular pentaquark systems with strangeness, we need to construct their wave functions. For these discussed $\Xi_c^{(\prime)} \bar{D}^{(*)}$ systems, their spin-orbital wave functions can be expressed as

$$|\Xi_c^{(\prime)} \bar{D}^{(2S+1)L_J}\rangle = \sum_{m, m_L} C_{\frac{1}{2}m, Lm_L}^{J, M} \chi_{\frac{1}{2}m} |Y_{L, m_L}\rangle, \quad (17)$$

$$|\Xi_c^{(\prime)} \bar{D}^{*(2S+1)L_J}\rangle = \sum_{m, m', m_S, m_L} C_{\frac{1}{2}m, 1m'}^{S, m_S} C_{S m_S, L m_L}^{J, M} \chi_{\frac{1}{2}m} \times \epsilon_{m'}^\mu |Y_{L, m_L}\rangle. \quad (18)$$

In the above expressions, the constant $C_{ab, cd}^{e, f}$ denotes the Clebsch-Gordan coefficient, and $|Y_{L, m_L}\rangle$ is the spherical harmonics function. The polarization vector ϵ_m^μ ($m = 0, \pm 1$) with spin-1 field is written as $\epsilon_\pm^\mu = (0, \pm 1, i, 0)/\sqrt{2}$ and $\epsilon_0^\mu = (0, 0, 0, -1)$ in the static limit, and the $\chi_{\frac{1}{2}m}$ stands for the spin wave function for the charmed baryons $\Xi_c^{(\prime)}$. And then, we summarize the flavor wave functions $|I, I_3\rangle$ for these discussed $\Xi_c^{(\prime)} \bar{D}^{(*)}$ systems in Table I.

TABLE I. Flavor wave functions for these discussed $\Xi_c^{(\prime)} \bar{D}^{(*)}$ systems. Here, I and I_3 are their isospins and the third components, respectively.

$ I, I_3\rangle$	Flavor wave functions
$ 1, 1\rangle$	$ \Xi_c^{(\prime)+} \bar{D}^{(*)0}\rangle$
$ 1, 0\rangle$	$\sqrt{\frac{1}{2}} \Xi_c^{(\prime)+} \bar{D}^{(*)-}\rangle + \sqrt{\frac{1}{2}} \Xi_c^{(\prime)0} \bar{D}^{(*)0}\rangle$
$ 1, -1\rangle$	$ \Xi_c^{(\prime)0} \bar{D}^{(*)-}\rangle$
$ 0, 0\rangle$	$\sqrt{\frac{1}{2}} \Xi_c^{(\prime)+} \bar{D}^{(*)-}\rangle - \sqrt{\frac{1}{2}} \Xi_c^{(\prime)0} \bar{D}^{(*)0}\rangle$

With the standard procedures of the OBE model, the expressions of the effective potentials in the coordinate space for these investigated isoscalar $\Xi_c^{(\prime)} \bar{D}_s^{(*)}$ systems are

given by

$$\begin{aligned}
\mathcal{V}^{\Xi_c \bar{D}} &= 2l_B g_\sigma Y_\sigma - \frac{3\beta\beta_B g_V^2}{4} Y_\rho + \frac{\beta\beta_B g_V^2}{4} Y_\omega, \\
\mathcal{V}^{\Xi_c' \bar{D}} &= -l_S g_\sigma Y_\sigma + \frac{3\beta\beta_S g_V^2}{8} Y_\rho - \frac{\beta\beta_S g_V^2}{8} Y_\omega, \\
\mathcal{V}^{\Xi_c \bar{D}^*} &= 2l_B g_\sigma \mathcal{A}_1 Y_\sigma - \frac{3\beta\beta_B g_V^2}{4} \mathcal{A}_1 Y_\rho + \frac{\beta\beta_B g_V^2}{4} \mathcal{A}_1 Y_\omega, \\
\mathcal{V}^{\Xi_c' \bar{D}^*} &= -l_S g_\sigma \mathcal{A}_1 Y_\sigma - \frac{g_1 g}{4f_\pi^2} [\mathcal{A}_2 \mathcal{O}_r + \mathcal{A}_3 \mathcal{P}_r] Y_\pi \\
&\quad - \frac{g_1 g}{36f_\pi^2} [\mathcal{A}_2 \mathcal{O}_r + \mathcal{A}_3 \mathcal{P}_r] Y_\eta \\
&\quad + \frac{3\beta\beta_S g_V^2}{8} \mathcal{A}_1 Y_\rho + \frac{3\lambda\lambda_S g_V^2}{18} [2\mathcal{A}_2 \mathcal{O}_r - \mathcal{A}_3 \mathcal{P}_r] Y_\rho \\
&\quad - \frac{\beta\beta_S g_V^2}{8} \mathcal{A}_1 Y_\omega - \frac{\lambda\lambda_S g_V^2}{18} [2\mathcal{A}_2 \mathcal{O}_r - \mathcal{A}_3 \mathcal{P}_r] Y_\omega.
\end{aligned}$$

Here, $\mathcal{O}_r = \frac{1}{r^2} \frac{\partial}{\partial r} r^2 \frac{\partial}{\partial r}$ and $\mathcal{P}_r = r \frac{\partial}{\partial r} \frac{1}{r} \frac{\partial}{\partial r}$. The function Y_i is defined as

$$Y_i \equiv \frac{e^{-m_i r} - e^{-\Lambda_i r}}{4\pi r} - \frac{\Lambda_i^2 - m_i^2}{8\pi\Lambda_i} e^{-\Lambda_i r}. \quad (19)$$

Additionally, we also define several operators, which include $\mathcal{A}_1 = \chi_3^\dagger (\epsilon_4^\dagger \cdot \epsilon_2) \chi_1$, $\mathcal{A}_2 = \chi_3^\dagger [\boldsymbol{\sigma} \cdot (i\epsilon_2 \times \epsilon_4^\dagger)] \chi_1$, and $\mathcal{A}_3 = \chi_3^\dagger T(\boldsymbol{\sigma}, i\epsilon_2 \times \epsilon_4^\dagger, \hat{\mathbf{r}}) \chi_1$. Here, the tensor force operator is expressed as $T(\boldsymbol{\sigma}, \mathbf{y}, \hat{\mathbf{r}}) = 3(\hat{\mathbf{r}} \cdot \boldsymbol{\sigma})(\hat{\mathbf{r}} \cdot \mathbf{y}) - \boldsymbol{\sigma} \cdot \mathbf{y}$ with $\hat{\mathbf{r}} = \mathbf{r}/|\mathbf{r}|$. In the effective potentials, the corresponding matrix elements $\langle f | \mathcal{A}_k | i \rangle$ can be obtained by these operators \mathcal{A}_k sandwiched between the relevant spin-orbit wave functions of the initial and final states. For example, the matrices element $\langle \Xi_c^{(\prime)} \bar{D}^* | \mathcal{A}_1 | \Xi_c^{(\prime)} \bar{D}^* \rangle$

with $J = 1/2$ can be expressed as $\begin{pmatrix} \mathcal{A}_1^{11} & \mathcal{A}_1^{12} \\ \mathcal{A}_1^{21} & \mathcal{A}_1^{22} \end{pmatrix}$ with

$$\begin{aligned}
\mathcal{A}_1^{11} &= \langle \Xi_c^{(\prime)} \bar{D}^* (^2\mathbb{S}_{\frac{1}{2}}) | \mathcal{A}_1 | \Xi_c^{(\prime)} \bar{D}^* (^2\mathbb{S}_{\frac{1}{2}}) \rangle, \\
\mathcal{A}_1^{12} &= \langle \Xi_c^{(\prime)} \bar{D}^* (^4\mathbb{D}_{\frac{1}{2}}) | \mathcal{A}_1 | \Xi_c^{(\prime)} \bar{D}^* (^2\mathbb{S}_{\frac{1}{2}}) \rangle, \\
\mathcal{A}_1^{21} &= \langle \Xi_c^{(\prime)} \bar{D}^* (^2\mathbb{S}_{\frac{1}{2}}) | \mathcal{A}_1 | \Xi_c^{(\prime)} \bar{D}^* (^4\mathbb{D}_{\frac{1}{2}}) \rangle, \\
\mathcal{A}_1^{22} &= \langle \Xi_c^{(\prime)} \bar{D}^* (^4\mathbb{D}_{\frac{1}{2}}) | \mathcal{A}_1 | \Xi_c^{(\prime)} \bar{D}^* (^4\mathbb{D}_{\frac{1}{2}}) \rangle.
\end{aligned}$$

In Table II, we collect the obtained relevant operator matrix elements $\langle f | \mathcal{A}_k | i \rangle$, which are used in our calculation.

When discussing the bound state properties of the S -wave isoscalar $\Xi_c \bar{D}^*$ states with $J^P = 1/2^-$ and $3/2^-$ after including the coupled channels $\Xi_c \bar{D}^*$ and $\Xi_c' \bar{D}^*$, we need the effective potentials in the coordinate space for

TABLE II. The relevant operator matrix elements $\langle f | \mathcal{A}_k | i \rangle$, which are obtained by sandwiching these operators between the relevant spin-orbit wave functions.

Spin	$J = 1/2$	$J = 3/2$
$\langle \Xi_c^{(\prime)} \bar{D}^* \mathcal{A}_1 \Xi_c^{(\prime)} \bar{D}^* \rangle$	$\begin{pmatrix} 1 & 0 \\ 0 & 1 \end{pmatrix}$	$\begin{pmatrix} 1 & 0 & 0 \\ 0 & 1 & 0 \\ 0 & 0 & 1 \end{pmatrix}$
$\langle \Xi_c' \bar{D}^* \mathcal{A}_2 \Xi_c' \bar{D}^* \rangle$	$\begin{pmatrix} -2 & 0 \\ 0 & 1 \end{pmatrix}$	$\begin{pmatrix} 1 & 0 & 0 \\ 0 & -2 & 0 \\ 0 & 0 & 1 \end{pmatrix}$
$\langle \Xi_c' \bar{D}^* \mathcal{A}_3 \Xi_c' \bar{D}^* \rangle$	$\begin{pmatrix} 0 & -\sqrt{2} \\ -\sqrt{2} & -2 \end{pmatrix}$	$\begin{pmatrix} 0 & 1 & 2 \\ 1 & 0 & -1 \\ 2 & -1 & 0 \end{pmatrix}$

the $\Xi_c \bar{D}^* \rightarrow \Xi_c' \bar{D}^*$ process, i.e.,

$$\begin{aligned}
\mathcal{V}^{\Xi_c \bar{D}^* \rightarrow \Xi_c' \bar{D}^*} &= -\frac{gg_4}{2\sqrt{6}f_\pi^2} [\mathcal{A}_2 \mathcal{O}_r + \mathcal{A}_3 \mathcal{P}_r] Y_{\pi 0} \\
&\quad + \frac{gg_4}{6\sqrt{6}f_\pi^2} [\mathcal{A}_2 \mathcal{O}_r + \mathcal{A}_3 \mathcal{P}_r] Y_{\eta 0} \\
&\quad - \frac{\lambda\lambda_I g_V^2}{\sqrt{6}} [2\mathcal{A}_2 \mathcal{O}_r - \mathcal{A}_3 \mathcal{P}_r] Y_{\rho 0} \\
&\quad + \frac{\lambda\lambda_I g_V^2}{3\sqrt{6}} [2\mathcal{A}_2 \mathcal{O}_r - \mathcal{A}_3 \mathcal{P}_r] Y_{\omega 0}.
\end{aligned}$$

Here, $m_0 = \sqrt{m^2 - q_0^2}$ and $\Lambda_0 = \sqrt{\Lambda^2 - q_0^2}$ with $q_0 = 0.06$ GeV.

III. THE CHARACTERISTIC MASS SPECTRA OF THE $\Xi_c^{(\prime)} \bar{D}^{(*)}$ MOLECULAR PENTAQUARKS

Based on the obtained effective potentials in the coordinate space for these discussed hidden-charm pentaquarks with strangeness, we can obtain the bound state solutions by solving the coupled channel Schrödinger equation, where the obtained bound state solutions mainly include the binding energy E , the root-mean-square radius r_{RMS} , and the probabilities for different components P_i , which may provide us the critical information to judge whether these discussed hidden-charm molecular pentaquark states with strangeness exist or not. In the coupled channel analysis, the probabilities for different components P_i are useful information to reflect the properties of the hadronic molecular states, except for the binding energy E and the root-mean-square radius r_{RMS} . If the coupled system is not dominant by the lowest mass threshold channel among the selected coupled channels, where usually the obtained root-mean-square radius r_{RMS} is too small, this coupled system is not recommended to be a hadronic molecular state (see Ref. [61] for more details).

Of course, when judging whether the loosely bound state is the possible hadronic molecular candidate, we also need to specify two points: (1) As a free parameter, the cutoff value of the form factor cannot be determined exactly due to the lack of relevant experiment data. In realistic calculation, one should find bound state solution by changing the cutoff value. According to the experience of studying the deuteron by the OBE model, the cutoff value should not be far away from 1 GeV [5, 72–74]. Furthermore, we can reproduce the masses of the observed three P_c states [63] and T_{cc} state [75] under the hadronic molecular picture when taking the cutoff values around 1 GeV. In the present work, we still take the cutoff range around 1 GeV to discuss the bound state properties of the S -wave isoscalar $\Xi_c^{(\prime)}\bar{D}^{(*)}$ systems; (2) The reasonable binding energy for the possible hadronic molecular candidate should be at most tens of MeV, and the corresponding typical size should be larger than the size of all the included component hadrons [61]. These criteria may provide useful hints to identify the hidden-charm molecular pentaquark candidates with strangeness.

In our calculation, the masses of these involved hadrons are $m_\sigma = 600.00$ MeV, $m_\pi = 137.27$ MeV, $m_\eta = 547.86$ MeV, $m_\rho = 775.26$, $m_\omega = 782.66$ MeV, $m_D = 1867.25$ MeV, $m_{D^*} = 2008.56$ MeV, $m_{\Xi_c} = 2469.08$ MeV, and $m_{\Xi_c'} = 2578.45$ MeV, which are taken from the Particle Data Group [76].

A. The characteristic mass spectrum of the $\Xi_c\bar{D}^{(*)}$ molecular pentaquarks

For the S -wave isoscalar $\Xi_c\bar{D}^{(*)}$ systems, we list the obtained bound state solutions by considering the S - D wave mixing effect in Table. III. For the S -wave isoscalar $\Xi_c\bar{D}$ state with $J^P = 1/2^-$, we obtain the bound state solution by setting the cutoff parameter Λ around 1.41 GeV. For the S -wave isoscalar $\Xi_c\bar{D}^*$ states with $J^P = 1/2^-$ and $3/2^-$, there exist the bound state solutions when the cutoff parameter is taken to be around 1.39 GeV. Here, the probabilities for the D -wave components are zero for these two states, since the contribution of the tensor forces from the S - D wave mixing effect disappears for the case of the isoscalar $\Xi_c\bar{D}^*$ interactions. In addition, there exists mass degeneration for the S -wave isoscalar $\Xi_c\bar{D}^*$ states with $J^P = 1/2^-$ and $3/2^-$ when adopting same cutoff value in the S - D wave mixing analysis.

In the above discussions, we indicate that these discussed S -wave isoscalar $\Xi_c\bar{D}^{(*)}$ systems can be viewed as the hidden-charm molecular pentaquark candidates with single strangeness within the OBE model by considering the S - D wave mixing effect. However, there exist mass degeneration for the S -wave isoscalar $\Xi_c\bar{D}^*$ states with $J^P = 1/2^-$ and $3/2^-$ when adopting same cutoff value in the S - D wave mixing analysis. Since the observation of the charmoniumlike state $X(3872)$, various corrections [5] including the coupled channel effect [77–79] have been introduced to discuss the fine properties of the hadron-

TABLE III. Bound state properties for the S -wave isoscalar $\Xi_c\bar{D}^{(*)}$ systems by considering the S - D wave mixing effect. Here, the cutoff Λ , binding energy E , and root-mean-square radius r_{RMS} are in units of GeV, MeV, and fm, respectively.

$\Xi_c\bar{D}(J^P = 1/2^-)$			
Λ	E	r_{RMS}	
1.41	-0.35	4.73	
1.61	-4.82	1.64	
1.79	-12.49	1.10	
$\Xi_c\bar{D}^*(J^P = 1/2^-)$			
Λ	E	r_{RMS}	$P(^2S_{1/2}/^4D_{1/2})$
1.39	-0.34	4.70	100.00 /o(0)
1.57	-4.71	1.63	100.00 /o(0)
1.74	-12.21	1.10	100.00 /o(0)
$\Xi_c\bar{D}^*(J^P = 3/2^-)$			
Λ	E	r_{RMS}	$P(^4S_{3/2}/^2D_{3/2}/^4D_{3/2})$
1.39	-0.34	4.70	100.00 /o(0)/o(0)
1.57	-4.71	1.63	100.00 /o(0)/o(0)
1.74	-12.21	1.10	100.00 /o(0)/o(0)

hadron interactions in the OBE model, which may decorate the bound state properties of hadronic molecular states [22, 33, 38, 39, 44, 47, 61, 63, 68, 75, 77–142].

For the $\Xi_c\bar{D}^{(*)}$ molecular systems, the authors of Refs. [39, 47] once presented a coupled channel analysis within the OBE model. Here, for the S -wave isoscalar $\Xi_c\bar{D}^*$ state with $J^P = 3/2^-$, the coupled channel effect is helpful to form this molecular state [39], since the cutoff value becomes smaller after including the coupled channel effect compared with the situation without considering the coupled channel effect. However, when discussing the isoscalar $\Xi_c\bar{D}^*$ state with $J^P = 1/2^-$ with a coupled channel analysis, a puzzling phenomenon appears [39], where a higher $\Xi_c'\bar{D}^*$ channel among these selected coupled channels becomes dominant. Obviously, a jump occurs which is not reasonable. The reason resulting in this puzzling phenomenon is that the author of Ref. [39] took the same cutoff value for these considered channels in their coupled channel analysis. Obviously, this treatment should be improved to ensure that the coupled channel effect only plays the role to decorate the discussed pure state, which was not realised in these early studies [39, 47, 61, 84, 87, 90–92].

An approaches to overcome such problem is proposed in this work. In practice, the cutoff values for the involved coupled channels can be different. Along this line, we discuss the bound state properties of the isoscalar $\Xi_c\bar{D}^*$ molecular states with $J^P = 1/2^-$ and $3/2^-$, where we adopt different cutoff values for the $\Xi_c\bar{D}^*$ and $\Xi_c'\bar{D}^*$ channels. In Table IV, we present the bound state solutions

of the S -wave isoscalar $\Xi_c \bar{D}^*$ states with $J^P = 1/2^-$ and $3/2^-$ by the coupled channel analysis. The above fact shows that the coupled channel effect indeed may decorate the bound state properties of the S -wave isoscalar $\Xi_c \bar{D}^*$ state with $J^P = 1/2^-$, and ensure that the jump phenomenon mentioned above does not happen. Thus, the conclusion of the existence of the S -wave isoscalar $\Xi_c \bar{D}^*$ molecular state with $J^P = 1/2^-$ does not change when considering the coupled channel effect. We should indicate that the former studies in Refs. [35, 44, 46] also support the existence of the S -wave isoscalar $\Xi_c \bar{D}^*$ molecular states with $J^P = 1/2^-$ and $3/2^-$. In this work, we can find the bound state solutions for the S -wave isoscalar $\Xi_c \bar{D}^*$ states with $J^P = 1/2^-$ and $3/2^-$, where the $\Xi_c \bar{D}^*$ is the dominant channel. Different from the case of the single channel analysis, there exists the mass difference for the S -wave isoscalar $\Xi_c \bar{D}^*$ states with $J^P = 1/2^-$ and $3/2^-$ when considering the coupled channel effect.

TABLE IV. Bound state properties for the S -wave isoscalar $\Xi_c \bar{D}^*$ system by performing the coupled channel analysis. Here, the cutoff Λ , binding energy E , and root-mean-square radius r_{RMS} are in units of GeV, MeV, and fm, respectively. Additionally, Λ and Λ' denote the cutoff parameters of the $\Xi_c \bar{D}^*$ and $\Xi'_c \bar{D}^*$ channels, respectively.

Λ	Λ'	E	r_{RMS}	$P(\Xi_c \bar{D}^*/\Xi'_c \bar{D}^*)$
$\Xi_c \bar{D}^*(J^P = 1/2^-)$				
1.12	0.92	-0.30	4.74	97.75/2.25
1.16	0.96	-4.33	1.58	89.46/10.54
1.20	1.00	-14.67	0.89	77.76/22.24
$\Xi_c \bar{D}^*(J^P = 3/2^-)$				
1.31	1.11	-0.29	4.87	99.73/0.27
1.43	1.23	-4.52	1.64	98.54/1.46
1.56	1.36	-15.01	0.98	96.48/3.52

We also need to mention that the $P_{cs}(4459)$ existing in the $J/\psi\Lambda$ invariant mass spectrum may be described by two peak structures with the masses of 4454.9 MeV and 4467.9 MeV [51]. According to Table IV, the masses of the S -wave isoscalar $\Xi_c \bar{D}^*$ state with $J^P = 1/2^-$ may be around 4454.9 MeV, we can reproduce this mass with the cutoff parameters of the $\Xi_c \bar{D}^*$ and $\Xi'_c \bar{D}^*$ channels respectively around 1.22 GeV and 1.02 GeV, which are close to the reasonable range around 1.00 GeV [70, 71, 80, 81]. Here, its binding energy and root-mean-square radius are -22.70 MeV and 0.73 fm, and the probabilities of the $\Xi_c \bar{D}^*$ and $\Xi'_c \bar{D}^*$ components are around 72% and 28%, respectively.

The corresponding thresholds of the $\Xi_c \bar{D}$ and $\Xi_c \bar{D}^*$ channels are 4336.33 MeV and 4477.64 MeV, so the masses of the S -wave isoscalar $\Xi_c \bar{D}^*$ states are larger than that of the S -wave isoscalar $\Xi_c \bar{D}$ state. Based on the analysis mentioned above, it is clear that the

masses of these discussed hidden-charm molecular pentaquarks with strangeness satisfy the relation $m[\Xi_c \bar{D}] < m[\Xi_c \bar{D}^*]$. Generally, the above analysis presents a characteristic mass spectrum of hidden-charm pentaquark with strangeness. Additionally, our obtained S -wave isoscalar $\Xi_c \bar{D}$ state with $J^P = 1/2^-$ has the mass lower than that of the observed $P_{\psi_s}^\Lambda(4338)$ [23]. However, the $P_{\psi_s}^\Lambda(4338)$ was reported in the $J/\psi\Lambda$ invariant mass spectrum via the $B^- \rightarrow J/\psi\Lambda\bar{p}$ process with the width about 7 MeV. Thus, there is still some possibility that the origin of the $P_{\psi_s}^\Lambda(4338)$ can be due to the S -wave isoscalar $\Xi_c \bar{D}$ molecular state with $J^P = 1/2^-$, which should be checked in future experiment. Especially, confirming it via the $\Xi_b^- \rightarrow J/\psi\Lambda K$ process is strongly suggested here.

In Ref. [143], the authors once estimated the probabilities of finding the $\Sigma_c \bar{D}^{(*)}$ and $J/\psi p$ components inside the P_c states within the effective range expansion and the resonance compositeness relations, and concluded that the weight of the $\Sigma_c \bar{D}^{(*)}$ component around 99% is much larger than that of the $J/\psi p$ component. Thus, most of the previous theoretical studies usually ignored the contribution of the $J/\psi p$ channel when explaining the observed P_c states as the S -wave isoscalar $\Sigma_c \bar{D}^{(*)}$ molecular states. Here, we would like to mention that there exists similar spectroscopy behavior for the S -wave isoscalar $\Sigma_c \bar{D}^{(*)}$ and $\Xi_c \bar{D}^{(*)}$ molecular states, which reflects that the weight of the $\Xi_c \bar{D}^{(*)}$ component should be much larger than that of the $J/\psi\Lambda$ component for these discussed hidden-charm molecular pentaquarks with single strangeness. In the present work, we do not consider the contribution of the $J/\psi\Lambda$ channel when discussing the bound state properties of the S -wave isoscalar $\Xi_c^{(\prime)} \bar{D}^{(*)}$ states.

B. The characteristic mass spectrum of the $\Xi_c^{(\prime)} \bar{D}^{(*)}$ molecular pentaquarks

Following the procedure discussed above, we present the binding energy, root-mean-square radius, and probabilities for different components for the S -wave isoscalar $\Xi_c^{(\prime)} \bar{D}^{(*)}$ systems in Fig. 2. For the S -wave isoscalar $\Xi_c \bar{D}$ state with $J^P = 1/2^-$, the bound state solution can be found when the cutoff parameter is fixed to be larger than 1.45 GeV. For the S -wave isoscalar $\Xi'_c \bar{D}^*$ system, the π , σ , η , ρ , and ω exchanges contribute to the total effective potentials. For the S -wave isoscalar $\Xi'_c \bar{D}^*$ state with $J^P = 1/2^-$, there exists the bound state solutions with the cutoff parameter around 0.92 GeV, while we can obtain loosely bound state solutions for the S -wave isoscalar $\Xi_c \bar{D}^*$ state with $J^P = 3/2^-$ when we tune the cutoff parameter to be around 1.63 GeV. Thus, we can conclude these discussed states are the isoscalar hidden-charm molecular pentaquark candidates with strangeness, which is consistent with the conclusions in Refs. [35, 44, 46, 47]. Additionally, the largest mass of these isoscalar hidden-charm molecular

pentaquark candidates with strangeness is the S -wave isoscalar $\Xi'_c \bar{D}^*$ state with $J^P = 3/2^-$, followed by the the S -wave isoscalar $\Xi'_c \bar{D}^*$ state with $J^P = 1/2^-$ and the S -wave isoscalar $\Xi'_c \bar{D}$ state with $J^P = 1/2^-$. Here, we need to point out that the masses of the S -wave isoscalar $\Xi'_c \bar{D}^*$ state with $J^P = 3/2^-$ and $1/2^-$ are 4582.3 MeV and 4568.7 MeV based on the chiral effective field theory [35], and the masses of the S -wave isoscalar $\Xi'_c \bar{D}^*$ state with $J^P = 3/2^-$ and $1/2^-$ are 4582.1 MeV and 4564.9 MeV with a quark level interaction [46], which are comparable with our results. For the $\Xi'_c \bar{D}^{(*)}$ pentaquark systems, there also exists a characteristic mass spectrum as predicted above (see Fig. 2).

$J^P = 1/2^-$			$J^P = 1/2^-$			
Λ	E	r_{RMS}	Λ	E	r_{RMS}	$P(^2S_{1/2}^4 D_{3/2})$
1.45	-0.29	4.92	0.92	-0.50	4.02	99.63/0.37
1.65	-4.62	1.65	0.97	-4.18	1.64	99.45/0.55
1.84	-12.14	1.10	1.02	-11.90	1.06	99.45/0.55

$\Xi'_c \bar{D}$ $\Xi'_c \bar{D}^*$

$J^P = 3/2^-$		$J^P = 3/2^-$				
Λ	E	r_{RMS}	$P(^2S_{3/2}^4 D_{3/2}^4 D_{3/2})$			
$\frac{1}{2}$	$\frac{1}{2}$	$\frac{3}{2}$	1.63	-0.33	4.87	98.49/0.17/1.18
$\frac{1}{2}$	$\frac{1}{2}$	$\frac{3}{2}$	2.09	-4.79	1.75	96.63/0.32/3.05
$\frac{1}{2}$	$\frac{1}{2}$	$\frac{3}{2}$	2.55	-12.42	1.21	95.65/0.35/4.00

$\Xi'_c \bar{D}$ $\Xi'_c \bar{D}^*$ $J^P = 3/2^-$

Characteristic spectrum

FIG. 2. Bound state properties for the S -wave isoscalar $\Xi'_c \bar{D}^{(*)}$ systems. Here, the cutoff Λ , binding energy E , and root-mean-square radius r_{RMS} are in units of GeV, MeV, and fm, respectively.

For the S -wave loosely bound state, its bound state properties have close relation to the effective potentials, where the S -wave interaction has dominant contribution. For the S -wave $\Xi'_c \bar{D}^*$ system, the operator \mathcal{A}_2 has connection to the interaction strength, i.e., $\langle \Xi'_c \bar{D}^* | \mathcal{A}_2 | \Xi'_c \bar{D}^* \rangle = -2$ and 1 with $J = 1/2$ and $3/2$, respectively. Thus, we may conclude that the cutoff value of the S -wave isoscalar $\Xi'_c \bar{D}^*$ state with $J^P = 1/2^-$ should be smaller than that of the S -wave isoscalar $\Xi'_c \bar{D}^*$ state with $J^P = 3/2^-$ if getting the same binding energy. For the S -wave $\Xi_c \bar{D}^*$ system, there only exists the operator \mathcal{A}_1 with $\langle \Xi_c \bar{D}^* | \mathcal{A}_1 | \Xi_c \bar{D}^* \rangle = 1$ for the cases of $J = 1/2$ and $3/2$. Therefore, the cutoff for the S -wave isoscalar $\Xi_c \bar{D}^*$ states with $J^P = 1/2^-$ and $3/2^-$ has the same value for getting the same binding energy when performing the S - D wave mixing analysis.

At present, there does not exist the experimental information involved in the coupling constant g_σ . Thus, we have to estimate the g_σ value by the phenomenological model. Usually, there are two determined values for coupling constant g_σ , which are 0.76 and 2.82, by the spontaneously broken chiral symmetry [64] and the quark model [62]. Both of them were adopted in realistic study. As

shown in Table V, the loosely bound state solutions can be obtained with the cutoff values closed to 1 GeV for the S -wave isoscalar $\Xi'_c \bar{D}^*$ state with $J^P = 1/2^-$ by taking either $g_\sigma = 0.76$ or $g_\sigma = 2.82$. The uncertainty resulted from the g_σ value can be compensated by smally changing Λ value. Thus, the conclusion of existing the S -wave isoscalar $\Xi'_c \bar{D}^*$ molecular state with $J^P = 1/2^-$ is still hold when considering the uncertainties of the coupling constant g_σ .

TABLE V. Bound state properties for the S -wave isoscalar $\Xi'_c \bar{D}^*$ state with $J^P = 1/2^-$ when considering the uncertainties of the coupling constant g_σ . Here, the cutoff Λ , binding energy E , and root-mean-square radius r_{RMS} are in units of GeV, MeV, and fm, respectively.

$g_\sigma = 0.76$			
Λ	E	r_{RMS}	$P(^2S_{1/2}^4 D_{3/2})$
0.92	-0.50	4.02	99.63 /0.37
0.97	-4.18	1.64	99.45 /0.55
1.02	-11.90	1.06	99.45 /0.55
$g_\sigma = 2.82$			
Λ	E	r_{RMS}	$P(^2S_{1/2}^4 D_{3/2})$
0.83	-0.33	4.62	99.71 /0.29
0.88	-3.94	1.74	99.53 /0.47
0.93	-11.95	1.11	99.51 /0.49

We should indicate that the $P_{cs}(4459)$ and $P_{\psi_s}^\Lambda(4338)$ are also close to the corresponding thresholds of baryon-meson channels like the combination of the $\Lambda_c/\Sigma_c^{(*)}$ baryon and the $D_s^{(*)}$ meson. Although the isovector $\Sigma_c^{(*)} \bar{D}_s^{(*)}$ channel cannot couple with the discussed isoscalar systems, the $\Lambda_c \bar{D}_s^{(*)}$ channel can interact with the discussed systems, which is not addressed in the present coupled channel analysis.

By above discussion, we may conclude that there exists the characteristic mass spectra of the S -wave isoscalar $\Xi_c^{(\prime)} \bar{D}^{(*)}$ -type hidden-charm molecular pentaquarks with single strangeness. In Fig. 3, we compare the masses between the observed hidden-charm pentaquarks with single strangeness [23, 51] and our predicted S -wave isoscalar $\Xi_c^{(\prime)} \bar{D}^{(*)}$ -type hidden-charm molecular pentaquarks with single strangeness.

In the following, we discuss the two-body hidden-charm decay behaviors of our predicted S -wave isoscalar $\Xi_c^{(\prime)} \bar{D}^{(*)}$ -type hidden-charm molecular pentaquarks with single strangeness, which is inspired by the observation from LHCb of the P_c and P_{cs} states [14, 23, 51, 144] via the two-body hidden-charm decay channels. In the past decades, the heavy quark symmetry was often used to discuss the properties of the hadrons which contain the heavy quarks. Thus, we may discuss the two-body hidden-charm decay behaviors of these predicted hidden-

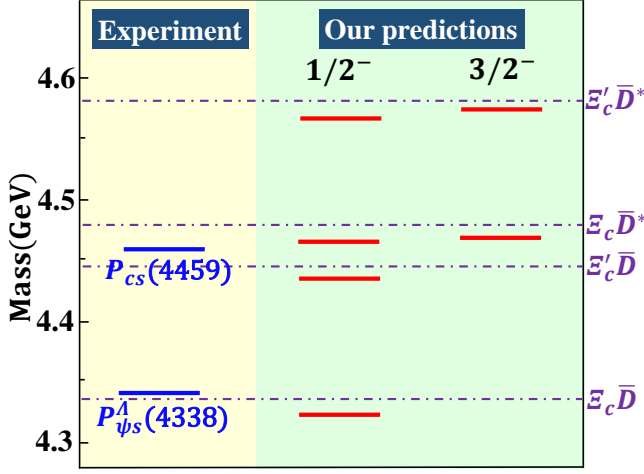


FIG. 3. The comparison of the masses between the observed hidden-charm pentaquarks with single strangeness [23, 51] and our predicted S -wave isoscalar $\Xi_c^{(\prime)}\bar{D}^{(*)}$ -type hidden-charm molecular pentaquarks with single strangeness. Here, the purple dash-dotted lines denote the thresholds of these discussed hidden-charm molecular pentaquarks with single strangeness, and the blue and red thick solid lines represent the masses of the observed hidden-charm pentaquarks with strangeness and our predicted S -wave isoscalar $\Xi_c^{(\prime)}\bar{D}^{(*)}$ -type hidden-charm molecular pentaquarks with single strangeness, respectively.

charm molecular pentaquarks with single strangeness within the heavy quark symmetry.

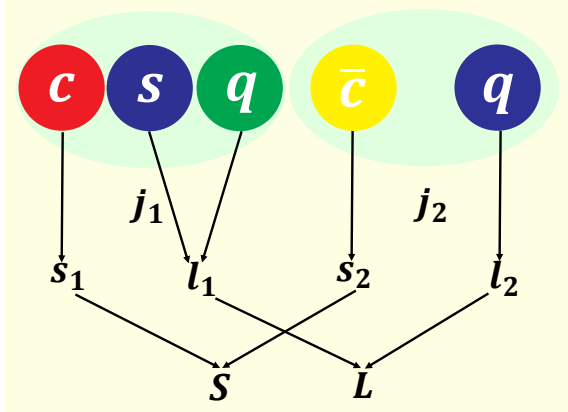


FIG. 4. Diagram for the calculation of the 9- j coefficients. Here, j_1 and j_2 denote the total angular momentum quantum numbers for the charmed baryons and anti-charmed mesons, respectively. s_1 and s_2 stand for the spin quantum numbers of the heavy quarks. l_1 and l_2 are the spin quantum numbers of the light quarks. And then, $l_1 = 0$ and 1 for the Ξ_c and Ξ_c' baryons, respectively.

As shown in Fig. 4, we expand the spin wave functions of the heavy hadron systems $|\ell_1 s_1 j_1, \ell_2 s_2 j_2, JM\rangle$ in terms of the heavy quark basis $|\ell_1 \ell_2 L, s_1 s_2 S, JM\rangle$,

where the general relation can be expressed as

$$|\ell_1 s_1 j_1, \ell_2 s_2 j_2, JM\rangle = \sum_{S,L} \hat{S} \hat{L} \hat{j}_1 \hat{j}_2 \begin{Bmatrix} \ell_1 & \ell_2 & L \\ s_1 & s_2 & S \\ j_1 & j_2 & J \end{Bmatrix} \times |\ell_1 \ell_2 L, s_1 s_2 S, JM\rangle \quad (20)$$

with $\hat{A} = \sqrt{2A+1}$. Thus, we obtain

$$|\Xi_c \bar{D}(J = \frac{1}{2})\rangle = \frac{1}{2} |S_{c\bar{c}} = 0, L_{sqq} = \frac{1}{2}, J = \frac{1}{2}\rangle + \frac{\sqrt{3}}{2} |S_{c\bar{c}} = 1, L_{sqq} = \frac{1}{2}, J = \frac{1}{2}\rangle, \quad (21)$$

$$|\Xi_c \bar{D}^*(J = \frac{1}{2})\rangle = \frac{\sqrt{3}}{2} |S_{c\bar{c}} = 0, L_{sqq} = \frac{1}{2}, J = \frac{1}{2}\rangle - \frac{1}{2} |S_{c\bar{c}} = 1, L_{sqq} = \frac{1}{2}, J = \frac{1}{2}\rangle, \quad (22)$$

$$|\Xi_c' \bar{D}(J = \frac{1}{2})\rangle = \frac{1}{2} |S_{c\bar{c}} = 0, L_{sqq} = \frac{1}{2}, J = \frac{1}{2}\rangle - \frac{1}{2\sqrt{3}} |S_{c\bar{c}} = 1, L_{sqq} = \frac{1}{2}, J = \frac{1}{2}\rangle + \sqrt{\frac{2}{3}} |S_{c\bar{c}} = 1, L_{sqq} = \frac{3}{2}, J = \frac{1}{2}\rangle, \quad (23)$$

$$|\Xi_c' \bar{D}^*(J = \frac{1}{2})\rangle = -\frac{1}{2\sqrt{3}} |S_{c\bar{c}} = 0, L_{sqq} = \frac{1}{2}, J = \frac{1}{2}\rangle + \frac{5}{6} |S_{c\bar{c}} = 1, L_{sqq} = \frac{1}{2}, J = \frac{1}{2}\rangle + \frac{\sqrt{2}}{3} |S_{c\bar{c}} = 1, L_{sqq} = \frac{3}{2}, J = \frac{1}{2}\rangle. \quad (24)$$

For these predicted isoscalar S -wave $\Xi_c^{(\prime)}\bar{D}^{(*)}$ -type hidden-charm molecular pentaquarks with single strangeness, the allowed two-body hidden-charm decay channels include the $J/\psi\Lambda$ and $\eta_c(1S)\Lambda$. In the heavy quark symmetry, we can estimate

$$\begin{aligned} \mathcal{R}_{\text{HQS}}^1 &= \frac{\Gamma[\Xi_c \bar{D}(1/2^-) \rightarrow \eta_c(1S)\Lambda]}{\Gamma[\Xi_c \bar{D}(1/2^-) \rightarrow J/\psi\Lambda]} = \frac{1}{3}, \\ \mathcal{R}_{\text{HQS}}^2 &= \frac{\Gamma[\Xi_c \bar{D}^*(1/2^-) \rightarrow \eta_c(1S)\Lambda]}{\Gamma[\Xi_c \bar{D}^*(1/2^-) \rightarrow J/\psi\Lambda]} = 3, \\ \mathcal{R}_{\text{HQS}}^3 &= \frac{\Gamma[\Xi_c' \bar{D}(1/2^-) \rightarrow \eta_c(1S)\Lambda]}{\Gamma[\Xi_c' \bar{D}(1/2^-) \rightarrow J/\psi\Lambda]} = 3, \\ \mathcal{R}_{\text{HQS}}^4 &= \frac{\Gamma[\Xi_c' \bar{D}^*(1/2^-) \rightarrow \eta_c(1S)\Lambda]}{\Gamma[\Xi_c' \bar{D}^*(1/2^-) \rightarrow J/\psi\Lambda]} = \frac{3}{25}. \end{aligned}$$

For the S -wave $\Xi_c \bar{D}^*$ and $\Xi_c' \bar{D}^*$ molecular states with $J^P = 3/2^-$, the $J/\psi\Lambda$ is the two-body hidden-charm decay channel via the S -wave coupling, while the $\eta_c(1S)\Lambda$ channel is suppressed since it is a D -wave interaction. By this effort, we can find several significant two-body hidden-charm decay channels for these predicted hidden-charm molecular pentaquarks with single strangeness, which may provide crucial information of searching for

these predicted pentaquarks in future experiment. Besides the strong decay behavior of these predicted pentaquarks, their radiative decay behavior has aroused the interest as given in Ref. [145].

IV. DISCUSSION AND CONCLUSION

Very recently, the LHCb Collaboration announced the observation of the $P_{\psi_s}^\Lambda(4338)$ in the $J/\psi\Lambda$ invariant mass spectrum of the $B^- \rightarrow J/\psi\Lambda\bar{p}$ process [23]. The $P_{\psi_s}^\Lambda(4338)$ associated with the previously reported evidence of the $P_{cs}(4459)$ by LHCb shows a molecular-type characteristic mass spectrum of hidden-charm pentaquark with strangeness. Before that, a molecular-type characteristic mass spectrum of hidden-charm pentaquark was observed by discovering the $P_c(4312)$, $P_c(4440)$, and $P_c(4457)$ in the $J/\psi p$ invariant mass spectrum of the $\Lambda_b \rightarrow J/\psi p K$ [14]. In this work, we indicate the similarity of two molecular-type characteristic mass spectra mentioned above.

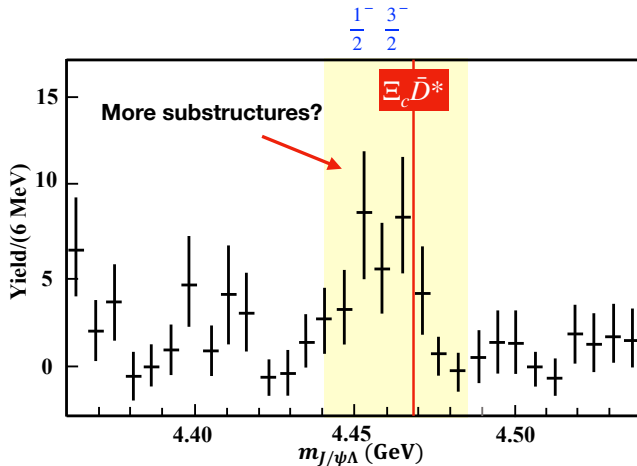


FIG. 5. The possible evidence of exiting substructures contained in the $P_{cs}(4459)$ enhancement structure. Here, the data of $J/\psi\Lambda$ invariant mass spectrum are from the LHCb [51]. The red solid line is the $\Xi_c\bar{D}^*$ threshold. Near this threshold, there should exist two $\Xi_c\bar{D}^*$ molecular states with $J^P = 1/2^-$ and $3/2^-$. The event cluster in the yellow ban shows possible double-peak evidence but it is not obvious, which can be tested by more precise data.

For quantitatively depicting this characteristic mass spectrum of hidden-charm pentaquark with strangeness, we apply the OBE model to obtain the interactions of the $\Xi_c\bar{D}^{(*)}$ systems, where the effective potentials of the focused systems can be deduced. By solving the Schrödinger equation, we find out the bound state solutions of the $\Xi_c\bar{D}^{(*)}$ pentaquark systems. The numerical result shows the existence of two $\Xi_c\bar{D}^*$ molecular pentaquarks with $J^P = 1/2^-$ and $3/2^-$, which can be related to the $P_{cs}(4459)$ structure. In fact, there exists a similar situation to the $P_c(4450)$, which was observed

firstly by LHCb in 2015 [144]. When reanalyzing more precise data of the $\Lambda_b \rightarrow J/\psi p K$ decay in 2019, LHCb indicated that the $P_c(4450)$ structure contains two substructures $P_c(4440)$ and $P_c(4457)$ [14]. We may conjecture that the double-peak phenomenon can be happened to the $P_{cs}(4459)$ structure¹ as illustrated in Fig. 5. Thus, we strongly suggest the experimental colleagues to reanalyze the $J/\psi\Lambda$ invariant mass spectrum of $\Xi_b^- \rightarrow J/\psi\Lambda K$ based on more precise data collected with the running of high-luminosity LHC.

If checking the resonant parameter of the reported $P_{\psi_s}^\Lambda(4338)$ [23], we cannot ignore a fact that the central value of the $P_{\psi_s}^\Lambda(4338)$ mass is a little bit larger than the threshold of the $\Xi_c\bar{D}$ channel. Thus, it seems unnatural to assign the $P_{\psi_s}^\Lambda(4338)$ as the $\Xi_c\bar{D}$ molecular state with $J^P = 1/2^-$ since the $\Xi_c\bar{D}$ molecular state has negative binding energy. As shown in Fig. 1, the mass gap between the $P_{cs}(4459)$ and the $P_{\psi_s}^\Lambda(4338)$ is smaller than that between the P_c states. If considering the similarity of the mass gap between the P_c states and that between the P_{cs} states. Taking the mass gap 137 MeV involved in the P_c states and the mass of the $P_{cs}(4459)$ as input, the P_{cs} partner of the $P_c(4312)$ should be located at 4322 MeV, which is lower than the observed $P_{\psi_s}^\Lambda(4338)$ by LHCb via the $B^- \rightarrow J/\psi\Lambda\bar{p}$ process. Thus, with more precise data, we also suggest to check such scenario in future experiment like LHCb. Here, a high-priority task is to confirm the observation of the $P_{\psi_s}^\Lambda(4338)$ by the $\Xi_b^- \rightarrow J/\psi\Lambda K$ process.

As a prediction, in this work we also give another molecular-type characteristic mass spectrum of hidden-charm $\Xi_c'\bar{D}^{(*)}$ pentaquark systems. Our result shows that there exist a $\Xi_c'\bar{D}$ molecular pentaquark with $J^P = 1/2^-$ and two $\Xi_c'\bar{D}^*$ molecular pentaquarks with $J^P = 1/2^-$ and $3/2^-$, which are near the thresholds of $\Xi_c'\bar{D}$ and $\Xi_c'\bar{D}^*$, respectively. Thus, searching for this predicted molecular-type characteristic mass spectrum of the $\Xi_c'\bar{D}^{(*)}$ pentaquark systems will be a new task for further experimental exploration of pentaquarks.

Note added.—When preparing the present paper, we noticed a similar work from Karliner and Rosner [146] appeared in arXiv. They also indicated the similarity of the mass gaps for these reported P_c and P_{cs} states. Different from Ref. [146], in this work we addressed a dynamical calculation within the OBE model to illustrate the importance of the molecular-type characteristic mass spectra of hidden-charm $\Xi_c^{(\prime)}\bar{D}^{(*)}$ pentaquark systems.

¹ In former experimental analysis [51], LHCb tried to fit the enhancement structure corresponding to the $P_{cs}(4459)$ by two substructures [51]. Due to the limit of precision of data, LHCb cannot make firm conclusion of the existence of substructure phenomenon [51].

ACKNOWLEDGEMENT

This work is supported by the China National Funds for Distinguished Young Scientists under Grant No.

11825503, National Key Research and Development Program of China under Contract No. 2020YFA0406400, the 111 Project under Grant No. B20063, and the National Natural Science Foundation of China under Grant No. 12175091.

-
- [1] M. Gell-Mann, A schematic model of baryons and mesons, *Phys. Lett.* **8**, 214 (1964).
- [2] G. Zweig, An SU(3) model for strong interaction symmetry and its breaking. Version 1, CERN, Report No. CERN-TH-401, 1964.
- [3] X. Liu, An overview of XYZ new particles, *Chin. Sci. Bull.* **59**, 3815 (2014).
- [4] A. Hosaka, T. Iijima, K. Miyabayashi, Y. Sakai, and S. Yasui, Exotic hadrons with heavy flavors: X , Y , Z , and related states, *Prog. Theor. Exp. Phys.* **2016**, 062C01 (2016).
- [5] H. X. Chen, W. Chen, X. Liu, and S. L. Zhu, The hidden-charm pentaquark and tetraquark states, *Phys. Rep.* **639**, 1 (2016).
- [6] J. M. Richard, Exotic hadrons: review and perspectives, *Few Body Syst.* **57**, 1185-1212 (2016).
- [7] R. F. Lebed, R. E. Mitchell and E. S. Swanson, Heavy-Quark QCD Exotica, *Prog. Part. Nucl. Phys.* **93** (2017), 143-194.
- [8] S. L. Olsen, T. Skwarnicki, and D. Zieminska, Non-standard heavy mesons and baryons: Experimental evidence, *Rev. Mod. Phys.* **90**, 015003 (2018).
- [9] F. K. Guo, C. Hanhart, U. G. Meißner, Q. Wang, Q. Zhao, and B. S. Zou, Hadronic molecules, *Rev. Mod. Phys.* **90**, 015004 (2018).
- [10] Y. R. Liu, H. X. Chen, W. Chen, X. Liu, and S. L. Zhu, Pentaquark and tetraquark states, *Prog. Part. Nucl. Phys.* **107**, 237 (2019).
- [11] N. Brambilla, S. Eidelman, C. Hanhart, A. Nefediev, C. P. Shen, C. E. Thomas, A. Vairo, and C. Z. Yuan, The XYZ states: Experimental and theoretical status and perspectives, *Phys. Rep.* **873**, 1 (2020).
- [12] L. Meng, B. Wang, G. J. Wang and S. L. Zhu, Chiral perturbation theory for heavy hadrons and chiral effective field theory for heavy hadronic molecules, arXiv:2204.08716.
- [13] H. X. Chen, W. Chen, X. Liu, Y. R. Liu and S. L. Zhu, An updated review of the new hadron states, arXiv:2204.02649.
- [14] R. Aaij *et al.* (LHCb Collaboration), Observation of a Narrow Pentaquark State, $P_c(4312)^+$, and of Two-Peak Structure of the $P_c(4450)^+$, *Phys. Rev. Lett.* **122**, 222001 (2019).
- [15] J. J. Wu, R. Molina, E. Oset and B. S. Zou, Prediction of narrow N^* and Λ^* resonances with hidden charm above 4 GeV, *Phys. Rev. Lett.* **105**, 232001 (2010).
- [16] W. L. Wang, F. Huang, Z. Y. Zhang, and B. S. Zou, $\Sigma_c \bar{D}$ and $\Lambda_c \bar{D}$ states in a chiral quark model, *Phys. Rev. C* **84**, 015203 (2011).
- [17] Z. C. Yang, Z. F. Sun, J. He, X. Liu, and S. L. Zhu, The possible hidden-charm molecular baryons composed of anti-charmed meson and charmed baryon, *Chin. Phys. C* **36**, 6 (2012).
- [18] J. J. Wu, T.-S. H. Lee, and B. S. Zou, Nucleon resonances with hidden charm in coupled-channel Models, *Phys. Rev. C* **85**, 044002 (2012).
- [19] X. Q. Li and X. Liu, A possible global group structure for exotic states, *Eur. Phys. J. C* **74**, 3198 (2014).
- [20] R. Chen, X. Liu, X. Q. Li, and S. L. Zhu, Identifying Exotic Hidden-Charm Pentaquarks, *Phys. Rev. Lett.* **115**, 132002 (2015).
- [21] M. Karliner and J. L. Rosner, New Exotic Meson and Baryon Resonances from Doubly-Heavy Hadronic Molecules, *Phys. Rev. Lett.* **115**, 122001 (2015).
- [22] T. J. Burns and E. S. Swanson, Production of P_c states in Λ_b decays, *Phys. Rev. D* **106**, no.5, 054029 (2022).
- [23] L. Collaboration (LHCb Collaboration), Observation of a $J/\psi\Lambda$ resonance consistent with a strange pentaquark candidate in $B^- \rightarrow J/\psi\Lambda\bar{p}$ decays, arXiv:2210.10346.
- [24] J. Hofmann and M. F. M. Lutz, Coupled-channel study of crypto-exotic baryons with charm, *Nucl. Phys. A* **763**, 90 (2005).
- [25] J. J. Wu, R. Molina, E. Oset and B. S. Zou, Dynamically generated N^* and Λ^* resonances in the hidden charm sector around 4.3 GeV, *Phys. Rev. C* **84**, 015202 (2011).
- [26] V. V. Anisovich, M. A. Matveev, J. Nyiri, A. V. Sarantsev, and A. N. Semenova, Nonstrange and strange pentaquarks with hidden charm, *Int. J. Mod. Phys. A* **30**, 1550190 (2015).
- [27] Z. G. Wang, Analysis of the $\frac{1}{2}^\pm$ pentaquark states in the diquark-diquark-antiquark model with QCD sum rules, *Eur. Phys. J. C* **76**, 142 (2016).
- [28] A. Feijoo, V. K. Magas, A. Ramos, and E. Oset, A hidden-charm $S = -1$ pentaquark from the decay of Λ_b into $J/\psi\eta\Lambda$ states, *Eur. Phys. J. C* **76**, no. 8, 446 (2016).
- [29] J. X. Lu, E. Wang, J. J. Xie, L. S. Geng, and E. Oset, The $\Lambda_b \rightarrow J/\psi K^0 \Lambda$ reaction and a hidden-charm pentaquark state with strangeness, *Phys. Rev. D* **93**, 094009 (2016).
- [30] H. X. Chen, L. S. Geng, W. H. Liang, E. Oset, E. Wang, and J. J. Xie, Looking for a hidden-charm pentaquark state with strangeness $S = -1$ from Ξ_b^- decay into $J/\psi K^- \Lambda$, *Phys. Rev. C* **93**, 065203 (2016).
- [31] R. Chen, J. He, and X. Liu, Possible strange hidden-charm pentaquarks from $\Sigma_c^{(*)} \bar{D}_s^*$ and $\Xi_c^{(*)} \bar{D}^*$ interactions, *Chin. Phys. C* **41**, 103105 (2017).
- [32] X. Z. Weng, X. L. Chen, W. Z. Deng and S. L. Zhu, Hidden-charm pentaquarks and P_c states, *Phys. Rev. D* **100**, no.1, 016014 (2019).
- [33] C. W. Xiao, J. Nieves, and E. Oset, Prediction of hidden charm strange molecular baryon states with heavy quark spin symmetry, *Phys. Lett. B* **799**, 135051 (2019).
- [34] C. W. Shen, H. J. Jing, F. K. Guo, and J. J. Wu, Exploring possible triangle singularities in the $\Xi_b^- \rightarrow K^- J/\psi\Lambda$ decay, *Symmetry* **12**, 1611 (2020).

- [35] B. Wang, L. Meng, and S. L. Zhu, Spectrum of the strange hidden charm molecular pentaquarks in chiral effective field theory, *Phys. Rev. D* **101**, 034018 (2020).
- [36] Q. Zhang, B. R. He, and J. L. Ping, Pentaquarks with the $qqs\bar{Q}Q$ configuration in the Chiral Quark Model, arXiv:2006.01042.
- [37] H. X. Chen, W. Chen, X. Liu and X. H. Liu, Establishing the first hidden-charm pentaquark with strangeness, *Eur. Phys. J. C* **81**, no.5, 409 (2021).
- [38] F. Z. Peng, M. J. Yan, M. Sánchez Sánchez and M. P. Valderrama, The $P_{cs}(4459)$ pentaquark from a combined effective field theory and phenomenological perspective, *Eur. Phys. J. C* **81**, no.7, 666 (2021).
- [39] R. Chen, Can the newly reported $P_{cs}(4459)$ be a strange hidden-charm $\Xi_c\bar{D}^*$ molecular pentaquark?, *Phys. Rev. D* **103**, no.5, 054007 (2021).
- [40] H. X. Chen, Hidden-charm pentaquark states through current algebra: from their production to decay*, *Chin. Phys. C* **46**, no.9, 093105 (2022).
- [41] M. Z. Liu, Y. W. Pan, and L. S. Geng, Can discovery of hidden charm strange pentaquark states help determine the spins of $P_c(4440)$ and $P_c(4457)$?, *Phys. Rev. D* **103**, 034003 (2021).
- [42] C. W. Xiao, J. J. Wu and B. S. Zou, Molecular nature of $P_{cs}(4459)$ and its heavy quark spin partners, *Phys. Rev. D* **103**, no.5, 054016 (2021).
- [43] M. L. Du, Z. H. Guo and J. A. Oller, Insights into the nature of the $P_{cs}(4459)$, *Phys. Rev. D* **104**, no.11, 114034 (2021).
- [44] J. T. Zhu, L. Q. Song and J. He, $P_{cs}(4459)$ and other possible molecular states from $\Xi_c^{(*)}\bar{D}^{(*)}$ and $\Xi_c'\bar{D}^{(*)}$ interactions, *Phys. Rev. D* **103**, no.7, 074007 (2021).
- [45] X. K. Dong, F. K. Guo and B. S. Zou, A survey of heavy-antiheavy hadronic molecules, *Progr. Phys.* **41**, 65-93 (2021).
- [46] K. Chen, R. Chen, L. Meng, B. Wang and S. L. Zhu, Systematics of the heavy flavor hadronic molecules, *Eur. Phys. J. C* **82**, no.7, 581 (2022).
- [47] R. Chen and X. Liu, Mass behavior of hidden-charm open-strange pentaquarks inspired by the established P_c molecular states, *Phys. Rev. D* **105**, no.1, 014029 (2022).
- [48] K. Chen, B. Wang and S. L. Zhu, Heavy flavor molecular states with strangeness, *Phys. Rev. D* **105**, no.9, 096004 (2022).
- [49] X. Hu and J. Ping, Investigation of hidden-charm pentaquarks with strangeness $S = -1$, *Eur. Phys. J. C* **82**, no.2, 118 (2022).
- [50] X. W. Wang and Z. G. Wang, Analysis of the $P_{cs}(4338)$ and related pentaquark molecular states via the QCD sum rules, arXiv:2207.06060.
- [51] R. Aaij *et al.* (LHCb Collaboration), Evidence of a $J/\psi\Lambda$ structure and observation of excited Ξ^- states in the $\Xi_b^- \rightarrow J/\psi\Lambda K^-$ decay, *Sci. Bull.* **66**, 1278-1287 (2021).
- [52] X. Wang, Z. F. Sun, D. Y. Chen, X. Liu and T. Matsuki, Non-strange partner of strangeonium-like state $Y(2175)$, *Phys. Rev. D* **85**, 074024 (2012).
- [53] H. Yukawa, On the Interaction of Elementary Particles I, *Proc. Phys. Math. Soc. Jap.* **17**, 48 (1935).
- [54] G. J. Ding, Are $Y(4260)$ and $Z_2^+(4250)$ D_1D or D_0D^* hadronic molecules? *Phys. Rev. D* **79**, 014001 (2009).
- [55] T. M. Yan, H. Y. Cheng, C. Y. Cheung, G. L. Lin, Y. C. Lin, and H. L. Yu, Heavy quark symmetry and chiral dynamics, *Phys. Rev. D* **46**, 1148 (1992); [*Phys. Rev. D* **55**, 5851E (1997)].
- [56] M. B. Wise, Chiral perturbation theory for hadrons containing a heavy quark, *Phys. Rev. D* **45**, R2188 (1992).
- [57] R. Casalbuoni, A. Deandrea, N. Di Bartolomeo, R. Gatto, F. Feruglio, and G. Nardulli, Light vector resonances in the effective chiral Lagrangian for heavy mesons, *Phys. Lett. B* **292**, 371 (1992).
- [58] R. Casalbuoni, A. Deandrea, N. Di Bartolomeo, R. Gatto, F. Feruglio, and G. Nardulli, Phenomenology of heavy meson chiral Lagrangians, *Phys. Rep.* **281**, 145 (1997).
- [59] M. Bando, T. Kugo and K. Yamawaki, Nonlinear Realization and Hidden Local Symmetries, *Phys. Rept.* **164**, 217 (1988).
- [60] M. Harada and K. Yamawaki, Hidden local symmetry at loop: A New perspective of composite gauge boson and chiral phase transition, *Phys. Rept.* **381**, 1 (2003).
- [61] R. Chen, A. Hosaka, and X. Liu, Searching for possible Ω_c -like molecular states from meson-baryon interaction, *Phys. Rev. D* **97**, 036016 (2018).
- [62] D. O. Riska and G. E. Brown, Nucleon resonance transition couplings to vector mesons, *Nucl. Phys. A* **679**, 577 (2001).
- [63] R. Chen, Z. F. Sun, X. Liu and S. L. Zhu, Strong LHCb evidence supporting the existence of the hidden-charm molecular pentaquarks, *Phys. Rev. D* **100**, no. 1, 011502 (2019).
- [64] W. A. Bardeen, E. J. Eichten and C. T. Hill, Chiral multiplets of heavy - light mesons, *Phys. Rev. D* **68**, 054024 (2003).
- [65] A. F. Falk and M. E. Luke, Strong decays of excited heavy mesons in chiral perturbation theory, *Phys. Lett. B* **292**, 119 (1992).
- [66] C. Isola, M. Ladisa, G. Nardulli, and P. Santorelli, Charming penguins in $B \rightarrow K^*\pi, K(\rho, \omega, \phi)$ decays, *Phys. Rev. D* **68**, 114001 (2003).
- [67] M. Cleven and Q. Zhao, Cross section line shape of $e^+e^- \rightarrow \chi_{c0}\omega$ around the $Y(4260)$ mass region, *Phys. Lett. B* **768**, 52 (2017).
- [68] Y. R. Liu and M. Oka, $\Lambda_c N$ bound states revisited, *Phys. Rev. D* **85**, 014015 (2012).
- [69] V. B. Berestetsky, E. M. Lifshitz, and L. P. Pitaevsky, *Quantum Electrodynamics*, 1982.
- [70] N. A. Tornqvist, From the deuteron to deusons, an analysis of deuteron-like meson-meson bound states, *Z. Phys. C* **61**, 525 (1994).
- [71] N. A. Tornqvist, On deusons or deuteron-like meson-meson bound states, *Nuovo Cim. Soc. Ital. Fis.* **107A**, 2471 (1994).
- [72] R. Machleidt, K. Holinde and C. Elster, The Bonn Meson Exchange Model for the Nucleon Nucleon Interaction, *Phys. Rept.* **149**, 1-89 (1987).
- [73] E. Epelbaum, H. W. Hammer and U. G. Meissner, Modern Theory of Nuclear Forces, *Rev. Mod. Phys.* **81**, 1773-1825 (2009).
- [74] A. Esposito, A. L. Guerrieri, F. Piccinini, A. Pilloni and A. D. Polosa, Four-Quark Hadrons: an Updated Review, *Int. J. Mod. Phys. A* **30**, 1530002 (2015).
- [75] N. Li, Z. F. Sun, X. Liu and S. L. Zhu, Perfect DD^* Molecular Prediction Matching the T_{cc} Observation at LHCb, *Chin. Phys. Lett.* **38**, no.9, 092001 (2021).
- [76] R. L. Workman *et al.* [Particle Data Group], Review of Particle Physics, *PTEP* **2022**, 083C01 (2022).

- [77] N. Li and S. L. Zhu, Hadronic Molecular States Composed of Heavy Flavor Baryons, *Phys. Rev. D* **86**, 014020 (2012).
- [78] N. Li and S. L. Zhu, Isospin breaking, Coupled-channel effects and Diagnosis of $X(3872)$, *Phys. Rev. D* **86**, 074022 (2012).
- [79] N. Li, Z. F. Sun, X. Liu and S. L. Zhu, Coupled-channel analysis of the possible $D^{(*)}D^{(*)}$, $\bar{B}^{(*)}\bar{B}^{(*)}$ and $D^{(*)}\bar{B}^{(*)}$ molecular states, *Phys. Rev. D* **88**, no.11, 114008 (2013).
- [80] R. Chen, A. Hosaka and X. Liu, Prediction of triple-charm molecular pentaquarks, *Phys. Rev. D* **96**, no.11, 114030 (2017).
- [81] F. L. Wang, R. Chen, Z. W. Liu, and X. Liu, Probing new types of P_c states inspired by the interaction between S -wave charmed baryon and anti-charmed meson in a \bar{T} doublet, *Phys. Rev. C* **101**, 025201 (2020).
- [82] R. Chen, X. Liu, Y. R. Liu and S. L. Zhu, Predictions of the hidden-charm molecular states with four-quark component, *Eur. Phys. J. C* **76**, no.6, 319 (2016).
- [83] R. Chen, F. L. Wang, A. Hosaka and X. Liu, Exotic triple-charm deuteronlike hexaquarks, *Phys. Rev. D* **97**, no.11, 114011 (2018).
- [84] F. L. Wang, R. Chen, Z. W. Liu and X. Liu, Possible triple-charm molecular pentaquarks from $\Xi_{cc}D_1/\Xi_{cc}D_2^*$ interactions, *Phys. Rev. D* **99**, no.5, 054021 (2019).
- [85] M. L. Du, V. Baru, F. K. Guo, C. Hanhart, U. G. Meißner, J. A. Oller and Q. Wang, Interpretation of the LHCb P_c States as Hadronic Molecules and Hints of a Narrow $P_c(4380)$, *Phys. Rev. Lett.* **124**, no.7, 072001 (2020).
- [86] Y. Yamaguchi, H. García-Tecocoatzi, A. Giachino, A. Hosaka, E. Santopinto, S. Takeuchi and M. Takizawa, P_c pentaquarks with chiral tensor and quark dynamics, *Phys. Rev. D* **101**, no.9, 091502 (2020).
- [87] F. L. Wang and X. Liu, Exotic double-charm molecular states with hidden or open strangeness and around 4.5 ~ 4.7 GeV, *Phys. Rev. D* **102**, no.9, 094006 (2020).
- [88] F. L. Wang, R. Chen and X. Liu, Prediction of hidden-charm pentaquarks with double strangeness, *Phys. Rev. D* **103**, no.3, 034014 (2021).
- [89] X. D. Yang, F. L. Wang, Z. W. Liu and X. Liu, Newly observed $X(4630)$: a new charmoniumlike molecule, *Eur. Phys. J. C* **81**, no.9, 807 (2021).
- [90] F. L. Wang and X. Liu, Investigating new type of doubly charmed molecular tetraquarks composed of charmed mesons in the H and T doublets, *Phys. Rev. D* **104**, no.9, 094030 (2021).
- [91] F. L. Wang, X. D. Yang, R. Chen and X. Liu, Hidden-charm pentaquarks with triple strangeness due to the $\Omega_c^{(*)}\bar{D}_s^{(*)}$ interactions, *Phys. Rev. D* **103**, no.5, 054025 (2021).
- [92] R. Chen, N. Li, Z. F. Sun, X. Liu and S. L. Zhu, Doubly charmed molecular pentaquarks, *Phys. Lett. B* **822**, 136693 (2021).
- [93] F. L. Wang, R. Chen and X. Liu, A new group of doubly charmed molecule with T -doublet charmed meson pair, *Phys. Lett. B* **835**, 137502 (2022).
- [94] M. L. Du, V. Baru, F. K. Guo, C. Hanhart, U. G. Meißner, J. A. Oller and Q. Wang, Revisiting the nature of the P_c pentaquarks, *JHEP* **08**, 157 (2021).
- [95] L. Roca, S. Sarkar, V. K. Magas and E. Oset, Unitary coupled channel analysis of the $\Lambda(1520)$ resonance, *Phys. Rev. C* **73**, 045208 (2006).
- [96] E. Oset and A. Ramos, Dynamically generated resonances from the vector octet-baryon octet interaction, *Eur. Phys. J. A* **44**, 445-454 (2010).
- [97] J. J. Xie and E. Oset, The DN , $\pi\Sigma_c$ interaction in finite volume and the $\Lambda_c(2595)$ resonance, *Eur. Phys. J. A* **48**, 146 (2012).
- [98] C. W. Xiao, J. Nieves and E. Oset, Combining heavy quark spin and local hidden gauge symmetries in the dynamical generation of hidden charm baryons, *Phys. Rev. D* **88**, 056012 (2013).
- [99] C. W. Xiao and E. Oset, Hidden beauty baryon states in the local hidden gauge approach with heavy quark spin symmetry, *Eur. Phys. J. A* **49**, 139 (2013).
- [100] A. Ozpineci, C. W. Xiao and E. Oset, Hidden beauty molecules within the local hidden gauge approach and heavy quark spin symmetry, *Phys. Rev. D* **88**, 034018 (2013).
- [101] W. H. Liang, C. W. Xiao and E. Oset, Baryon states with open beauty in the extended local hidden gauge approach, *Phys. Rev. D* **89**, no.5, 054023 (2014).
- [102] L. Roca, J. Nieves and E. Oset, LHCb pentaquark as a $\bar{D}^*\Sigma_c - \bar{D}^*\Sigma_c^*$ molecular state, *Phys. Rev. D* **92**, no.9, 094003 (2015).
- [103] G. Moir, M. Peardon, S. M. Ryan, C. E. Thomas and D. J. Wilson, Coupled-Channel $D\pi$, $D\eta$ and $D_s\bar{K}$ Scattering from Lattice QCD, *JHEP* **10**, 011 (2016).
- [104] X. W. Kang and J. A. Oller, P -wave coupled-channel scattering of $B_s\pi$, $B_s^*\pi$, $B\bar{K}$, $B^*\bar{K}$ and the puzzling $X(5568)$, *Phys. Rev. D* **94**, no.5, 054010 (2016).
- [105] M. Albaladejo, J. Nieves, E. Oset, Z. F. Sun and X. Liu, Can $X(5568)$ be described as a $B_s\pi$, $B\bar{K}$ resonant state?, *Phys. Lett. B* **757**, 515-519 (2016).
- [106] Y. Shimizu, D. Suenaga and M. Harada, Coupled channel analysis of molecule picture of $P_c(4380)$, *Phys. Rev. D* **93**, no.11, 114003 (2016).
- [107] Y. Shimizu and M. Harada, Hidden Charm Pentaquark $P_c(4380)$ and Doubly Charmed Baryon $\Xi_{cc}^*(4380)$ as Hadronic Molecule States, *Phys. Rev. D* **96**, no.9, 094012 (2017).
- [108] Y. Yamaguchi and E. Santopinto, Hidden-charm pentaquarks as a meson-baryon molecule with coupled channels for $\bar{D}^{(*)}\Lambda_c$ and $\bar{D}^{(*)}\Sigma_c^{(*)}$, *Phys. Rev. D* **96**, no.1, 014018 (2017).
- [109] J. X. Lu, X. L. Ren and L. S. Geng, $B_s\pi$ - $B\bar{K}$ interactions in finite volume and $X(5568)$, *Eur. Phys. J. C* **77**, no.2, 94 (2017).
- [110] Y. Shimizu, Y. Yamaguchi and M. Harada, Heavy quark spin multiplet structure of $\bar{P}^{(*)}\Sigma_Q^{(*)}$ molecular states, *Phys. Rev. D* **98**, no.1, 014021 (2018).
- [111] R. Pavao and E. Oset, Coupled channels dynamics in the generation of the $\Omega(2012)$ resonance, *Eur. Phys. J. C* **78**, no.10, 857 (2018).
- [112] T. Sekihara, Y. Kamiya and T. Hyodo, $N\Omega$ interaction: meson exchanges, inelastic channels, and quasi-bound state, *Phys. Rev. C* **98**, no.1, 015205 (2018).
- [113] M. P. Valderrama, $\Omega(2012)$ as a hadronic molecule, *Phys. Rev. D* **98**, no.5, 054009 (2018).
- [114] J. M. Dias, V. R. Debastiani, J. J. Xie and E. Oset, Doubly charmed Ξ_{cc} molecular states from meson-baryon interaction, *Phys. Rev. D* **98**, no.9, 094017 (2018).
- [115] J. He, H. Huang, D. Y. Chen and X. Zhu, Hidden-strange molecular states and the $N\phi$ bound states via

- a QCD van der Waals force, Phys. Rev. D **98**, no.9, 094019 (2018).
- [116] J. He and D. Y. Chen, $Z_c(3900)/Z_c(3885)$ as a virtual state from $\pi J/\psi - \bar{D}^* D$ interaction, Eur. Phys. J. C **78**, no.2, 94 (2018).
- [117] C. W. Shen, D. Rönchen, U. G. Meißner and B. S. Zou, Exploratory study of possible resonances in heavy meson - heavy baryon coupled-channel interactions, Chin. Phys. C **42**, no.2, 023106 (2018).
- [118] G. Montaña, A. Feijoo and À. Ramos, A meson-baryon molecular interpretation for some Ω_c excited states, Eur. Phys. J. A **54**, no.4, 64 (2018).
- [119] L. Meng, B. Wang, G. J. Wang and S. L. Zhu, The hidden charm pentaquark states and $\Sigma_c \bar{D}^{(*)}$ interaction in chiral perturbation theory, Phys. Rev. D **100**, no.1, 014031 (2019).
- [120] P. C. Bruns and A. Cieply, Coupled channels approach to ηN and $\eta' N$ interactions, Nucl. Phys. A **992**, 121630 (2019).
- [121] B. Yang, L. Meng and S. L. Zhu, Hadronic molecular states composed of spin- $\frac{3}{2}$ singly charmed baryons, Eur. Phys. J. A **55**, no.2, 21 (2019).
- [122] Q. X. Yu, J. M. Dias, W. H. Liang and E. Oset, Molecular Ξ_{bc} states from meson-baryon interaction, Eur. Phys. J. C **79**, no.12, 1025 (2019).
- [123] T. J. Burns and E. S. Swanson, Molecular interpretation of the $P_c(4440)$ and $P_c(4457)$ states, Phys. Rev. D **100**, no.11, 114033 (2019).
- [124] C. W. Xiao, J. Nieves and E. Oset, Heavy quark spin symmetric molecular states from $\bar{D}^{(*)}\Sigma_c^{(*)}$ and other coupled channels in the light of the recent LHCb pentaquarks, Phys. Rev. D **100**, no.1, 014021 (2019).
- [125] Q. X. Yu, R. Pavao, V. R. Debastiani and E. Oset, Description of the Ξ_c and Ξ_b states as molecular states, Eur. Phys. J. C **79**, no.2, 167 (2019).
- [126] Z. L. Wang and B. S. Zou, $\rho\rho$ scattering revisited with coupled channels of pseudoscalar mesons, Phys. Rev. D **99**, no.9, 096014 (2019).
- [127] P. G. Ortega, J. Segovia, D. R. Entem and F. Fernández, The Z_c structures in a coupled-channels model, Eur. Phys. J. C **79**, no.1, 78 (2019).
- [128] J. T. Zhu, S. Y. Kong, Y. Liu and J. He, Hidden-bottom molecular states from $\Sigma_b^{(*)} B^{(*)} - \Lambda_b B^{(*)}$ interaction, Eur. Phys. J. C **80**, no.11, 1016 (2020).
- [129] B. Yang, L. Meng and S. L. Zhu, Possible molecular states composed of doubly charmed baryons with coupled-channel effect, Eur. Phys. J. A **56**, no.2, 67 (2020).
- [130] R. Chen and Q. Huang, $Z_{cs}(3985)^-$: A strange hidden-charm tetraquark resonance or not?, Phys. Rev. D **103**, no.3, 034008 (2021).
- [131] R. Chen, Q. Huang, X. Liu and S. L. Zhu, Predicting another doubly charmed molecular resonance $T_{cc}^{\prime+}(3876)$, Phys. Rev. D **104**, no.11, 114042 (2021).
- [132] N. Ikeno, R. Molina and E. Oset, The $Z_{cs}(3985)$ as a threshold effect from the $\bar{D}_s^* D + \bar{D}_s D^*$ interaction, Phys. Lett. B **814**, 136120 (2021).
- [133] N. Yalikhun, Y. H. Lin, F. K. Guo, Y. Kamiya and B. S. Zou, Coupled-channel effects of the $\Sigma_c^{(*)} \bar{D}^{(*)} - \Lambda_c(2595) \bar{D}$ system and molecular nature of the P_c pentaquark states from one-boson exchange model, Phys. Rev. D **104**, no.9, 094039 (2021).
- [134] W. Hao, Y. Lu and B. S. Zou, Coupled channel effects for the charmed-strange mesons, Phys. Rev. D **106**, no.7, 074014 (2022).
- [135] N. Ikeno, R. Molina and E. Oset, Z_{cs} states from the $D_s^* \bar{D}$ and $J/\psi K^*$ coupled channels: Signal in $B^+ \rightarrow J/\psi \phi K^*$ decay, Phys. Rev. D **105**, no.1, 014012 (2022).
- [136] Y. Kamiya, T. Hyodo and A. Ohnishi, Femtoscopic study on DD^* and $D\bar{D}^*$ interactions for T_{cc} and $X(3872)$, Eur. Phys. J. A **58**, no.7, 131 (2022).
- [137] L. R. Dai, E. Oset, A. Feijoo, R. Molina, L. Roca, A. M. Torres and K. P. Khemchandani, Masses and widths of the exotic molecular $B_{(s)}^{(*)} B_{(s)}^{(*)}$ states, Phys. Rev. D **105**, no.7, 074017 (2022).
- [138] J. T. Zhu, S. Y. Kong, L. Q. Song and J. He, Systematical study of Ω_c -like molecular states from interactions $\Xi_c^{(*)} \bar{K}^{(*)}$ and $\Xi^{(*)} D^{(*)}$, Phys. Rev. D **105**, no.9, 094036 (2022).
- [139] Z. L. Wang, C. W. Shen, D. Rönchen, U. G. Meißner and B. S. Zou, Resonances in heavy meson-heavy baryon coupled-channel interactions, Eur. Phys. J. C **82**, no.5, 497 (2022).
- [140] N. Yalikhun and B. S. Zou, Anticharmed strange pentaquarks from the one-boson-exchange model, Phys. Rev. D **105**, no.9, 094026 (2022).
- [141] M. Albaladejo, T_{cc}^+ coupled channel analysis and predictions, Phys. Lett. B **829**, 137052 (2022).
- [142] B. Wang and S. L. Zhu, How to understand the $X(2900)$?, Eur. Phys. J. C **82**, no.5, 419 (2022).
- [143] Z. H. Guo and J. A. Oller, Anatomy of the newly observed hidden-charm pentaquark states: $P_c(4312)$, $P_c(4440)$ and $P_c(4457)$, Phys. Lett. B **793**, 144-149 (2019).
- [144] R. Aaij *et al.* (LHCb Collaboration), Observation of J/ψ Resonances Consistent with Pentaquark States in $\Lambda_b^0 \rightarrow J/\psi K^- p$ Decays, Phys. Rev. Lett. **115**, 072001 (2015).
- [145] F. L. Wang, H. Y. Zhou, Z. W. Liu and X. Liu, What can we learn from the electromagnetic properties of hidden-charm molecular pentaquarks with single strangeness?, Phys. Rev. D **106**, no.5, 054020 (2022).
- [146] M. Karliner and J. L. Rosner, New strange pentaquarks, Phys. Rev. D **106**, no.3, 036024 (2022).